The EMBO Journal Vol. 20 No. 8 pp. 1952–1962, 2001

Embryonic lethality and fetal liver apoptosis in mice lacking the c-*raf-1* gene

Mario Mikula, Martin Schreiber[1], Zvenislava Husak, Lucia Kucerova, Jochen Rüth, Rotraud Wieser[2], Kurt Zatloukal[3], Hartmut Beug[4], Erwin F.Wagner[4] and Manuela Baccarini[5]

Department of Cell- and Microbiology, Institute of Microbiology and Genetics and [4]Research Institute of Molecular Pathology, Vienna Biocenter, 1030 Vienna and [3]Department of Pathology, University of Graz, A-8036 Graz, Austria

[1]Present address: Department of Obstetrics and Gynecology, University of Vienna, Währinger Gürtel 18–20, A-1090 Vienna, Austria
[2]Present address: Department of Medical Biology, University of Vienna, Währinger Straße 10, A-1090 Vienna, Austria

[5]Corresponding author
e-mail: manuela@gem.univie.ac.at

The Raf kinases play a key role in relaying signals elicited by mitogens or oncogenes. Here, we report that c-*raf-1*$^{-/-}$ embryos are growth retarded and die at midgestation with anomalies in the placenta and in the fetal liver. Although hepatoblast proliferation does not appear to be impaired, c-*raf-1*$^{-/-}$ fetal livers are hypocellular and contain numerous apoptotic cells. Similarly, the poor proliferation of Raf-1$^{-/-}$ fibroblasts and hematopoietic cells cultivated *in vitro* is due to an increase in the apoptotic index of these cultures rather than to a cell cycle defect. Furthermore, Raf-1-deficient fibroblasts are more sensitive than wild-type cells to specific apoptotic stimuli, such as actinomycin D or Fas activation, but not to tumor necrosis factor-α. MEK/ERK activation is normal in Raf-1-deficient cells and embryos, and is probably mediated by B-Raf. These results indicate that the essential function of Raf-1 is to counteract apoptosis rather than to promote proliferation, and that effectors distinct from the MEK/ERK cascade must mediate the anti-apoptotic function of Raf-1.
Keywords: apoptosis/development/gene inactivation/MAP kinase/proliferation

Introduction

Cytosolic serine/threonine kinases convert extracellular stimuli into specific regulatory events affecting the pattern of gene expression, probably via phosphorylation of specific transcription factors. These kinases are often organized in cascades, a set-up that ensures signal modulation and amplification. The basic arrangement includes a small G-protein working upstream of a core module consisting of three kinases: a mitogen-activated protein (MAP) kinase kinase kinase (MAPKKK) that phosphorylates and activates a MAP kinase kinase (MAPKK), which in turn activates MAP kinase (MAPK). Activated Raf is the MAPKKK that regulates the ERK pathway, by phosphorylating and activating MEK. Within the MAPK cascade, Raf interacts physically with MEK-1 via its kinase domain and with GTP-loaded Ras via its N-terminus (Gu *et al*., 1994). Activated Ras binds to Raf with high affinity and mediates its translocation from the cytosol to the plasma membrane, where activation occurs via a complex, yet incompletely defined mechanism involving phosphorylation (Marshall, 1995; McCormick, 1995). Both Ras and Raf are proto-oncogenes. Thus, Raf represents an important intermediate in the transduction of regulated and deregulated proliferative signals (Naumann *et al*., 1997), and an attractive target for novel therapies aimed at interfering with its activation process and at eventually reversing its deregulated functions. Raf is a family of three serine/threonine-specific kinases (A-Raf, B-Raf and Raf-1) ubiquitously expressed throughout embryonic development. The three Raf isoforms are regulated differentially by upstream activators and exhibit quantitative differences in their ability to activate MEK (Marais *et al*., 1997), their best studied downstream substrate (Morrison and Cutler, 1997; Schaeffer and Weber, 1999).

A-*raf*- and B-*raf*-deficient mice have been generated. Newborn A-*raf*$^{-/-}$ mice and B-*raf*$^{-/-}$ embryos are growth retarded, confirming the positive role of Raf kinases in cell proliferation suggested by cell culture experiments. However, while B-*raf*-deficient embryos die at midgestation because of vascular defects due to apoptotic death of differentiated endothelial cells (Wojnowski *et al*., 1997), A-*raf*-deficient mice show neurological and intestinal defects, depending on the genetic background (Pritchard *et al*., 1996). These divergent phenotypes show that Raf isoforms can not always compensate for each other and that they serve distinct functions in different tissues.

The ubiquitously expressed c-*raf-1* is certainly the best studied, but probably least understood Raf isoform. Mutation of c-*raf-1* in the mouse, yielding an aberrant 62 kDa protein with residual kinase activity, results in embryonic or perinatal lethality, depending on the genetic background. The mutant embryos are growth retarded and display a rather complex phenotype with defects in the placenta, skin and lungs (Wojnowski *et al*., 1998).

Here, we report the generation of a null mutation in the c-*raf-1* gene in the mouse, which yields a recessive lethal phenotype. The embryos are growth retarded and die progressively around midgestation (E11.5–E13.5) with defects in the placenta and in the liver. The fetal liver is hypocellular and contains numerous apoptotic cells. *In vitro* studies with fibroblasts and hematopoietic cells confirmed that the non-redundant function of Raf-1 is to inhibit apoptosis, rather than to promote proliferation. ERK activation is not affected in Raf-1-deficient cells and

embryos, indicating that the phenotypes observed are due to lack of activation of Raf-1-specific effectors distinct from the ERK pathway.

Results

Disruption of the c-raf-1 gene

To inactivate the c-*raf-1* gene, we constructed a vector containing *loxP* sites 5′ and 3′ of exon 3. A third *loxP* site as well as selection markers (a neomycin resistance gene for positive selection and the HSV thymidine kinase gene for negative selection) were inserted upstream of the floxed exon 3 (Figure 1A). The mutation was introduced into E14.1 embryonic stem (ES) cells by homologous recombination, and exon 3 and the *Neo/TK* gene cassette were then deleted by transiently expressing Cre. Positive clones were identified by Southern blot analysis (Figure 1B). Germline-transmitting chimeras were obtained and bred to 129/Sv and C57BL/6 mice. Offspring and implants were genotyped by PCR analysis (Figure 1C). The excision of exon 3 resulted in the complete loss of Raf-1, as shown by western blot analysis of primary c-*raf-1*$^{-/-}$ fibroblasts (Figure 1D). This result was confirmed using antibodies directed against the N- and C-terminal regions of Raf-1 (data not shown). Consistently, these cells were devoid of Raf-1 kinase activity, as determined by immune complex kinase assays (Figure 1E).

Phenotype of c-raf-1$^{-/-}$ embryos

No viable c-*raf-1*$^{-/-}$ offspring were born from heterozygous (c-*raf-1*$^{+/-}$) intercrosses; therefore, c-*raf-1* is essential for mouse development. To assess the time of death, we collected and genotyped conceptuses at earlier times in development. This analysis was carried out on an inbred 129/Sv background as well as on a mixed 129BL/6 background. The viability plot (Figure 2A) shows a progressive decrease in the percentage of c-*raf-1*$^{-/-}$ embryos from day 11.5 (E11.5) until E16.5. The window of lethality was broader on a mixed background, but none of the mutants survived past E16.5. c-*raf-1*$^{-/-}$ fetuses could be distinguished from their littermates starting from E11.5. The mutant fetuses of both inbred 129/Sv and mixed 129BL/6 background were smaller (~20% weight reduction by E12.5; Figure 2B and data not shown) than wild-type or heterozygous littermates, and were developmentally retarded. Mutant placentas of both inbred 129/Sv and mixed 129BL/6 background were also smaller than those of wild-type or heterozygous littermates (~20% weight reduction by E12.5). Histological examination revealed that both the spongiotrophoblast and the labyrinth layer of the c-*raf-1*$^{-/-}$ placentas were reduced in size. In particular, the labyrinth layer was poorly vascularized and contained abundant mesenchymal cells (Figure 2B and C and data not shown). These anomalies may affect the exchange of gases and nutrients between the fetus and the mother, thereby contributing to midgestational death.

Increased apoptosis in c-raf-1$^{-/-}$ fetal livers

In addition to their small size, a characteristic feature of the c-*raf-1*$^{-/-}$ fetuses was that their vasculature was less obvious and that they were paler than their littermates (Figure 2B). In particular, the mutant livers were very pale

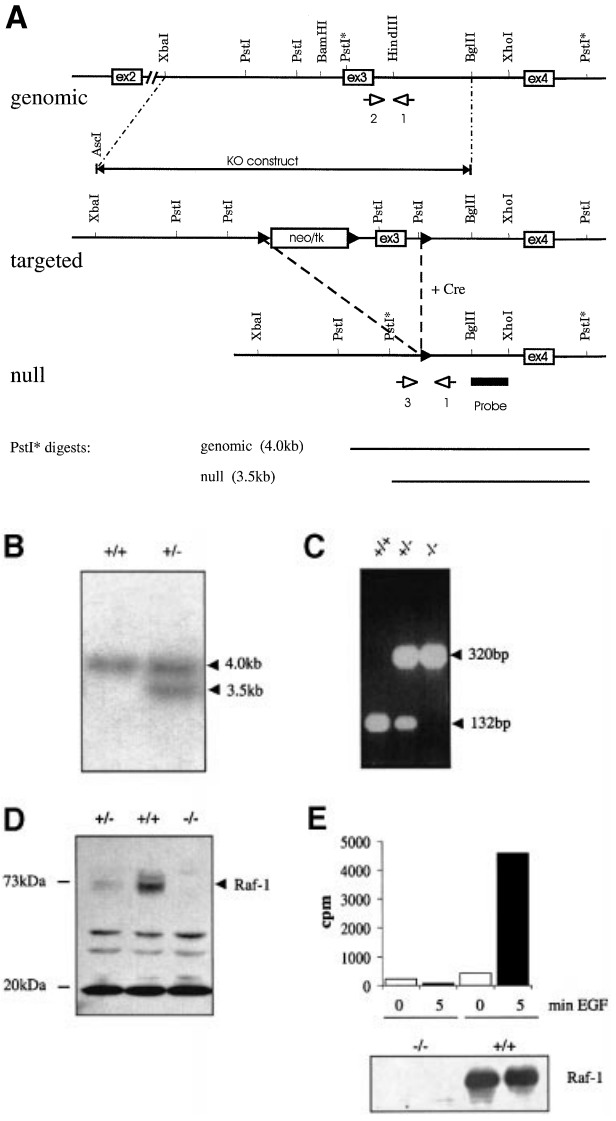

Fig. 1. Targeting of the mouse c-*raf-1* gene. (**A**) Schematic representation of the targeting strategy. Genomic, genomic locus before recombination; targeted, homologously recombined targeting vector; null, targeted locus after Cre-mediated removal of exon 3 and of the *Neo*/*TK* cassette. The targeting vector contained *loxP* sites (triangles) 5′ and 3′ of exon 3 of the c-*raf-1* gene as well as selection markers positioned between two *loxP* sites upstream of the floxed exon 3. The *Pst*I sites delimiting the diagnostic fragments obtained by digesting the genomic and mutated c-*raf-1* alleles are marked with an asterisk. Open arrows indicate the positions of the PCR primers 1, 2 and 3 used for genotyping. (**B**) Southern blot analysis of *Pst*I-digested genomic DNA from a targeted ES cell clone. The probe used is indicated in (A). (**C**) PCR analysis of DNA isolated from E12.5 fetuses using the indicated primers. (**D**) Western blot of whole-cell lysates from MEFs using an antibody that recognizes the Raf kinase domain. (**E**) Immune complex kinase assay of Raf-1 immunoprecipitates from control (+/+) and Raf-1-deficient (–/–) fibroblasts untreated or stimulated with EGF (5 min, 33 nM). One representative experiment out of three is shown.

and significantly reduced in size. Histological examination revealed that the mutant liver was hypocellular compared with those of normal littermates, and that the sinuses contained fewer red blood cells (Figure 3A). In addition, cell size was slightly larger in the mutant embryos (Figure 3). This phenotype was observed in seven out of

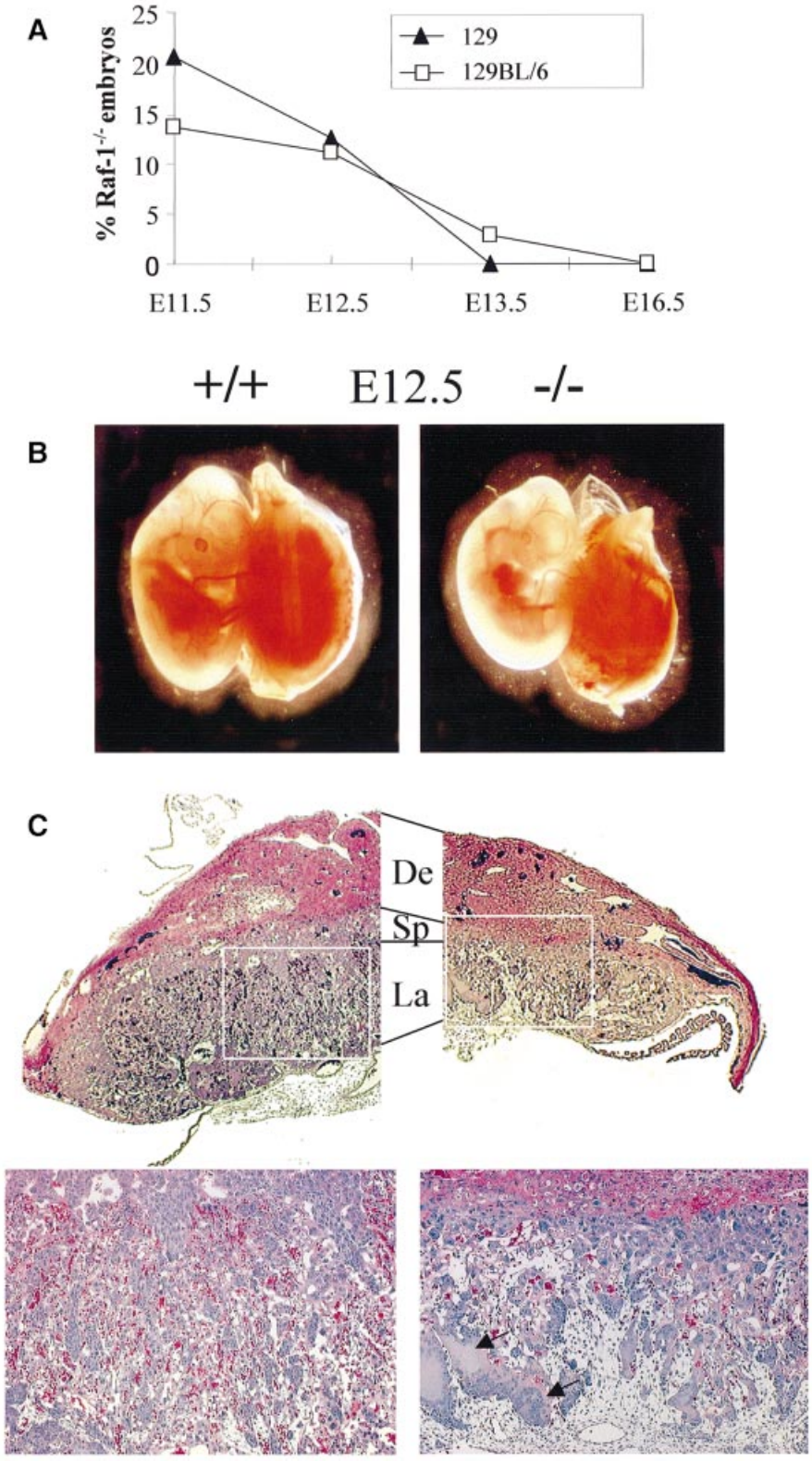

Fig. 2. c-*raf-1* inactivation is lethal at midgestation. (**A**) The percentage recovery of c-*raf-1*$^{-/-}$ conceptuses (of total viable embryos recovered from c-*raf-1*$^{+/-}$ intercrosses) is shown as a function of gestational age. Two hundred embryos of either background were genotyped. (**B**) Phenotype of a c-*raf-1*$^{-/-}$ fetus (right) and a control littermate (left) of 129/sv background at E12.5. c-*raf-1*$^{-/-}$ fetuses are smaller, developmentally retarded and paler than their normal littermates. The fetuses are shown with the placenta attached. (**C**) Placental defects in c-*raf-1*$^{-/-}$ mice. Radial sections of an E12.5 placenta from a wild-type (+/+) and a c-*raf-1*$^{-/-}$ littermate (–/–) of 129/sv background are shown. In the –/– placenta, the labyrinth layer (La) and the spongiotrophoblast layer (Sp) are reduced in size compared with +/+ controls. In addition, the labyrinth layer of the –/– placenta is less vascularized. In contrast, the decidua (De) appears normal. The lower panels show a higher magnification of the boxed areas. Note the mesenchymal cells that predominate in the –/– labyrinth layer (arrows).

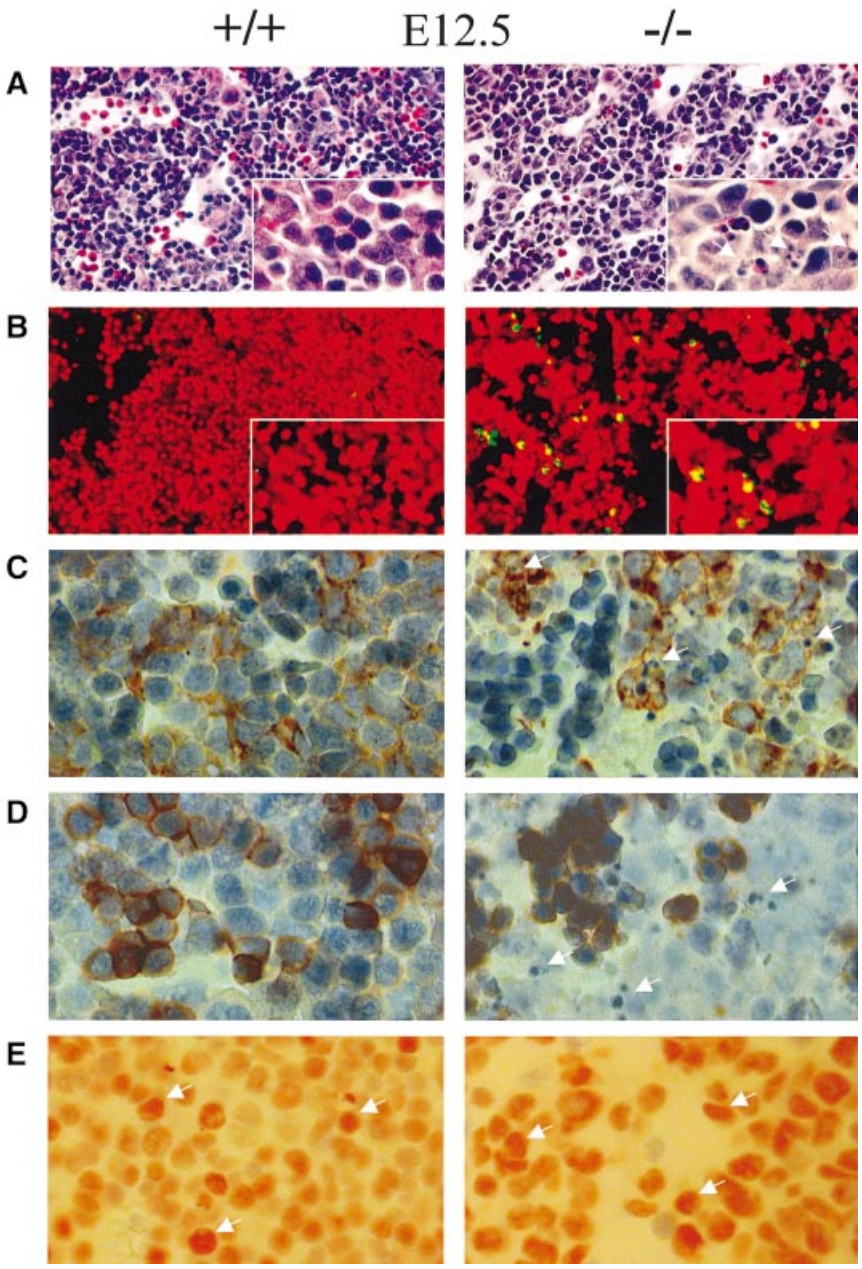

Fig. 3. Fetal liver defects in E12.5 c-*raf-1*$^{-/-}$ embryos. (**A**) Parasagittal section through the fetal liver of a c-*raf-1*$^{-/-}$ embryo (–/–) and of a littermate control (+/+) of 129/sv background. Note the hypocellularity and the abundance of pyknotic nuclei in the –/– livers. The boxed areas show higher magnifications of the fetal livers. (**B**) TUNEL analysis on sections from the same fetal livers shown in (A). Note the significant numbers of positively stained cells in the –/– liver. Sections were stained with propidium iodide to visualize the nuclei. (C and D) Immunohistochemical analysis of the fetal liver. The cell types undergoing apoptosis were characterized using rabbit polyclonal antibodies to keratins 8 and 18 to visualize hepatoblasts (**C**) and the erythroid-specific TER119 antibody (**D**). Note the presence of pyknotic and fragmented nuclei (white arrows) in keratin 8/18-positive and in TER119-negative cells of the –/– fetal liver. (**E**) *In situ* staining for the expression of PCNA; 81% of the wild-type and 88% of the –/– liver cells express PCNA, indicating that they are actively cycling.

seven fetuses analyzed, of both inbred 129/Sv and mixed 129BL/6 background. Five of these seven mutant fetal livers contained large numbers of pyknotic and fragmented nuclei (Figure 3A). This morphology is typically associated with apoptosis. *In situ* end-labeling of DNA (TUNEL) confirmed elevated apoptosis in mutant livers (Figure 3B). The cell type affected was characterized by immunohistochemical staining using antibodies against keratins 8 and 18 (expressed in hepatoblasts) and against TER119 (erythroid specific). Pyknotic nuclei were found mainly in keratin 8- and keratin 18-positive and TER119-negative cells (Figure 3C and D). Thus, apoptosis in c-*raf-1*$^{-/-}$ fetal livers appears to be associated mainly with the hepatoblast compartment.

To ascertain whether a proliferation defect contributed to liver hypocellularity, we performed *in situ* staining for expression of proliferating cell nuclear antigen (PCNA). Most of the hepatoblasts had entered the cell cycle and expressed PCNA in both c-*raf-1*$^{-/-}$ embryos and normal littermates (Figure 3E).

Analysis of c-raf-1$^{-/-}$ hematopoietic cells

The above data imply that the anemic appearance of the fetuses might be due to the failure of the hepatoblasts to support hematopoiesis. It should be noted, however, that cells in the advanced stages of apoptosis may lose surface markers, and therefore negative results obtained by immunohistochemical staining are not conclusive. To assess directly whether the hematopoietic cells had a cell-autonomous survival defect, we established cultures of multipotent hematopoietic precursors from c-*raf-1*$^{-/-}$ and wild-type fetal livers in a serum-free medium (StemPro34), supplemented with stem cell factor (SCF), flk2/flt 3 ligand, interleukin (IL)-3, IL-6, granulocyte–macrophage colony-stimulating factor (GM-CSF) and dexamethasone. c-*raf-1*$^{-/-}$ fetal livers yielded low amounts of cells (1.96×10^6 compared with 14.7×10^6 obtained from +/+ littermates). These cells could be maintained in culture for up to 10 days. At this time, a total of 4530×10^6 cells had been generated from a single +/+ fetal liver, yielding a 308-fold net increase in cell number. Heterozygous livers yielded similar results. In contrast, only 121×10^6 multipotent cells could be recovered from the c-*raf-1*$^{-/-}$ fetal liver (61.7-fold net increase; Figure 4A). The experiment was repeated twice using single fetal livers or pools of three, with similar results. In Raf-1$^{-/-}$ cultures, the number of S-phase cells was only slightly reduced compared with wild type, but the number of apoptotic cells was increased significantly (Figure 4B; 17.46% as compared with 3.14% in wild-type cultures). Thus, the increase in spontaneous apoptosis most probably accounts for the defect observed.

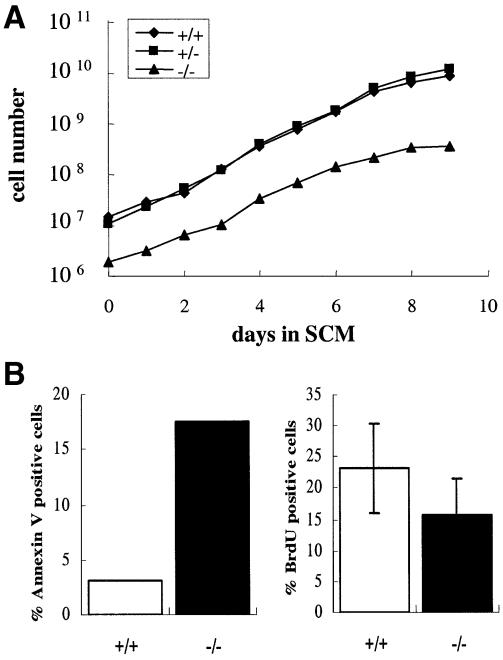

Fig. 4. Analysis of c-*raf-1*$^{-/-}$ hematopoietic cells in culture. Fetal livers were isolated on E11.5 from wild-type (+/+) and homozygous c-*raf-1*$^{-/-}$ (–/–) littermates of mixed 129BL/6 background. Cells were pre-cultured in media supporting the expansion of hematopoietic cells for 8 days to enrich for multipotent hematopoietic precursors. (**A**) Multipotent precursors of each genotype were seeded at a density of 2×10^6 cells/ml, further cultivated and counted at daily intervals. Cells were maintained at a constant density of 2×10^6 cells/ml. The plot shows the total number of cells generated per fetal liver as a function of the time in culture. (**B**) Percentage of annexin V-positive (left panel) or BrdU-positive (right panel) cells in asynchronous cultures (day 8) of hematopoietic fetal livers cells from wild-type (+/+, open bars) and c-*raf-1*$^{-/-}$ (–/–, closed bars) littermates. A representative experiment out of two is shown.

Increased apoptosis in c-raf-1$^{-/-}$ embryonic fibroblasts

The data reported above show that c-*raf-1*$^{-/-}$ fetal liver cells cultured *in vitro* fail to accumulate and are more prone than wild-type cells to undergo apoptosis. We next established primary fibroblasts from c-*raf-1*$^{-/-}$ fetuses. The morphology and size of the mutant fibroblasts were indistinguishable from those of wild-type cells. However, the numbers of mutant cells obtained from these cultures were significantly lower compared with heterozygous or wild-type controls (Figure 5A). In addition, c-*raf-1*$^{-/-}$ fibroblasts showed lower saturation densities than wild-type cells at all serum concentrations, ranging from 5 to 30% (~70% of controls). The saturation densities of mutant and wild-type fibroblasts increased proportionally with serum concentration. Thus, the mutant cells are still able to respond to growth factors, albeit to a reduced extent (Figure 5B). Raf-1$^{-/-}$ fibroblasts could be immortalized, although they underwent prolonged crisis (data not shown). If cell proliferation was affected, the lack of Raf-1 should delay G_1 to S progression during the cell cycle. However, fluorescence-activated cell sorting (FACS) analysis of asynchronous cells revealed that G_1, S and G_2 cell cycle phases were distributed similarly in c-*raf-1*$^{-/-}$ and wild-type fibroblasts (Figure 5C and D). To confirm this observation, we synchronized primary fibroblasts in G_0 by density arrest and growth factor withdrawal, and measured the percentage of cells with a DNA content >2N after serum stimulation. Both c-*raf-1*$^{-/-}$ and wild-type fibroblasts exited G_1 with the same kinetics. As a control, wild-type fibroblasts failed to progress through the cell cycle in the presence of a MEK inhibitor (Figure 5E).

The FACS profiles of continuously growing cultures showed an increased number of cells with a sub-2N DNA content in Raf-1$^{-/-}$ fibroblasts as compared with wild type (Figure 5C and D; 5.26 versus 2.43%), suggesting increased apoptosis in the G_1 phase. The consequences of Raf-1 inactivation for fibroblast turnover were assessed directly by determining simultaneously the number of cells in S phase [by bromodeoxyuridine (BrdU) labeling] and the number of apoptotic cells (by TUNEL staining). Consistent with the results summarized above, the number of S-phase cells in wild-type and mutant cultures was indistinguishable. The number of apoptotic cells in the Raf-1$^{-/-}$ cultures, however, was clearly elevated as compared with wild type (Figure 5F; $8.65 \pm 3.20\%$ in mutant versus $1.83 \pm 0.02\%$ in wild-type cultures). Thus, the reduced cell yield of c-*raf-1*$^{-/-}$ cultures correlates with an increase in apoptosis, but not with a cell cycle defect.

In addition, primary Raf-1$^{-/-}$ fibroblasts were more susceptible than wild type to apoptosis induced by growth factor deprivation and actinomycin D treatment (Figure 5G, left panel). Raf-1$^{-/-}$ fibroblasts immortalized according to the 3T3 protocol lost their hypersensitivity towards actinomycin D (Figure 5G, right panel), but were more susceptible than wild-type cells to Fas activation.

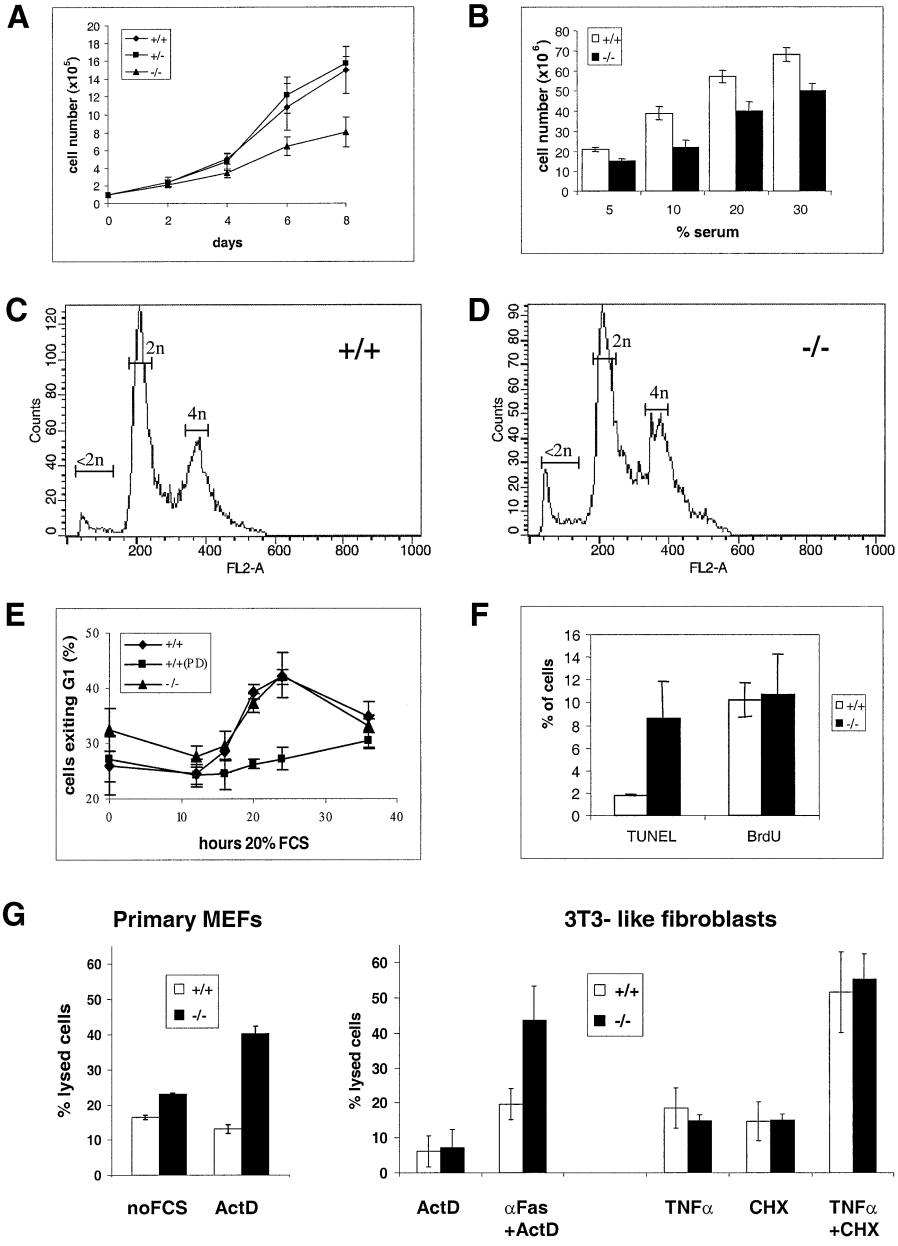

Fig. 5. Characterization of c-*raf-1*$^{-/-}$ fibroblast cultures. (**A**) Proliferation curves of wild-type (+/+), c-*raf-1*$^{+/-}$ (+/–) and c-*raf-1*$^{-/-}$ (–/–) primary fibroblasts. The average ± SD numbers of cells isolated from two individual littermates of each genotype are shown, each determined in triplicate. (**B**) Saturation density analysis of wild-type (+/+, open bars) and c-*raf-1*$^{-/-}$ (–/–, closed bars) primary fibroblasts as a function of serum concentration. Cells were counted after 14 days of culture in the presence of the indicated concentrations of FCS. The average ± SD numbers of cells isolated from two individual littermates of each genotype are shown, each determined in triplicate. (**C** and **D**) Representative FACS profiles of continuosly growing control (+/+) and c-*raf-1*$^{-/-}$ (–/–) primary fibroblasts. Asynchronous cells were stained with propidium iodide and their DNA content was determined by FACS analysis. (**E**) Quantitative analysis of G_1/S-phase progression in wild-type (+/+) primary fibroblasts, untreated or treated with the MEK inhibitor PD 98059 (50 μM, throughout the duration of the experiment) and c-*raf-1*$^{-/-}$ (–/–) primary fibroblasts. The percentage of cells exiting G_1 (i.e. the percentage of cells in S, G_2 or M) at the indicated times after serum stimulation of G_0-synchronized cells (see Materials and methods) was quantified by propidium iodide staining and FACS analysis. (**F**) Percentage of BrdU-incorporating and TUNEL-positive cells in parallel asynchronous cultures of primary wild-type (+/+, open bars) and Raf-1$^{-/-}$ (–/–, closed bars) fibroblasts. The data represent the mean value of cells isolated from two individual littermates of each genotype, and vertical bars represent the range of the samples. (**G**) Effect of different apoptosis-inducing stimuli on fibroblasts from wild-type (open bars) and c-*raf-1*$^{-/-}$ (closed bars) littermates. Primary fibroblasts (left panel) were serum starved or treated with 20 ng/ml actinomycin D (ActD) for 24 h. 3T3-like cells (right panel) were treated with 20 ng/ml actinomycin D and 50 ng/ml hamster anti-mouse Fas antibody for 22 h, or with 100 ng/ml murine TNF-α, 5 μg/ml cycloheximide (CHX) or a combination of both for 12 h. Cell death was assessed by measuring lactate dehydrogenase release. Primary fibroblasts or 3T3-like cells isolated from three individual littermates of each genotype were used in the experiment, and the data shown represent the mean ± SD.

In contrast, 3T3-like Raf-1-deficient cells were resistant to the cytotoxic effects of tumor necrosis factor-α (TNF-α) alone, and they were not more susceptible than the wild type to a combined treatment with TNF-α and cycloheximide. Therefore, Raf-1 inactivation appears to cause hypersensitivity to selective apoptotic stimuli.

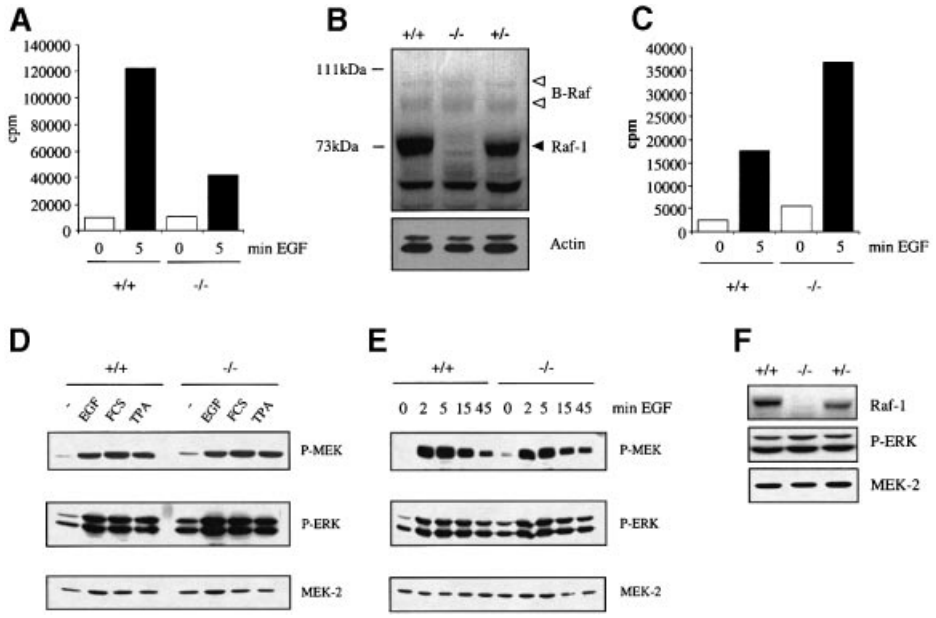

Fig. 6. Activation of the ERK pathway and of the B-Raf kinase in c-*raf-1*$^{-/-}$ fibroblasts. (**A**) The MEK kinase activity present in whole-cell lysates of untreated or EGF-stimulated (33 nM, 5 min) wild-type (+/+) or c-*raf-1*$^{-/-}$ (–/–) primary fibroblasts was measured in a coupled assay. (**B**) Raf immunoblot of whole-cell lysates from wild-type (+/+), c-*raf-1*$^{+/-}$ (+/–) or c-*raf-1*$^{-/-}$ (–/–) primary fibroblasts. The antibody used was raised against the Raf kinase domain and recognizes all three Raf proteins, albeit with different efficiency (Raf-1 >> B-Raf >> A-Raf; Kolch *et al*., 1990). An actin immunoblot is shown as a loading control. (**C**) Kinase activity of B-Raf immunoprecipitates measured in a coupled assay. The amounts of B-Raf contained in the immunoprecipitates were equal, as determined by immunoblotting (not shown). The results are expressed as c.p.m. incorporated into the substrate. One representative experiment out of three is shown. (D and E) Wild-type (+/+) and c-*raf-1*$^{-/-}$ (–/–) primary fibroblasts were stimulated for 10 min with EGF (33 nM), FCS (10%) or TPA (5 μM) (**D**), or with 33 nM EGF for different time periods (**E**) prior to cell lysis. The presence of the phosphorylated, active forms of MEK (pMEK) and ERK (pERK), as well as of MEK2 as a loading control, was detected by immunoblotting with the corresponding antibodies. (**F**) ERK phosphorylation in lysates from wild-type (+/+), c-*raf-1*$^{+/-}$ (+/–) or c-*raf-1*$^{-/-}$ (–/–) embryos. A Raf-1 immunoblot is shown as a genotype control and a MEK-2 immunoblot is shown as a loading control.

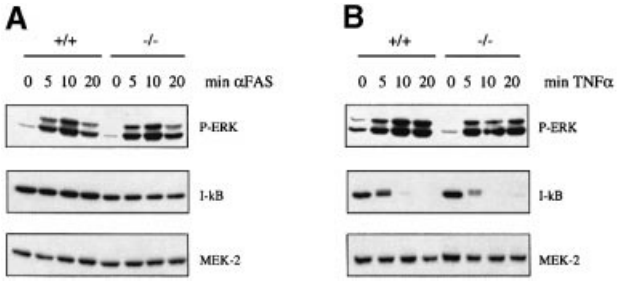

Fig. 7. ERK phosphorylation and I-κB degradation in c-*raf-1*$^{-/-}$ fibroblasts treated with anti-Fas antibody or TNF-α. Wild-type (+/+) and c-*raf-1*$^{-/-}$ (–/–) primary fibroblasts were stimulated with 50 ng/ml hamster anti-mouse Fas antibody (**A**) or 100 ng/ml TNF-α (**B**) for different time periods prior to cell lysis. The presence of the phosphorylated, active forms of ERK (pERK), as well as of I-κB or of the loading control MEK2, was detected by immunoblotting with the corresponding antibodies.

Activation of the ERK pathway and I-κB degradation are unaffected in c-raf-1$^{-/-}$ *fibroblasts*

We next investigated whether the inactivation of c-*raf-1* had any effect on the ERK pathway. Epidermal growth factor (EGF)-stimulated MEK kinase activity was still present in whole-cell lysates of Raf-1$^{-/-}$ fibroblasts, but it was strongly reduced (~30% of wild type; Figure 6A). These data indicate that Raf-1 represents a major fraction of the cellular MEK kinase activity *in vitro*, and that its loss is not compensated by the up-regulation of other MEK kinases. B-Raf is expressed at a much lower level than Raf-1 in fibroblasts, and compensatory overexpression was not observed in Raf-1$^{-/-}$ cells (Figure 6B). However, the basal as well as the EGF-stimulated activity of B-Raf were elevated (2-fold) in Raf-1-deficient fibroblasts compared with wild-type cells (Figure 6C). Activation of MEK and MAPK was normal in Raf-1$^{-/-}$ fibroblasts treated with a variety of extracellular stimuli (Figure 6D). The responses to EGF (Figure 6E), analyzed in more detail, showed the same intensity and kinetics of stimulation in wild-type and mutant cells. Furthermore, lysates of whole c-*raf-1*$^{-/-}$, c-*raf-1*$^{+/-}$ and c-*raf-1*$^{+/+}$ littermate embryos contained indistinguishable amounts of phosphorylated ERK (Figure 6F). Thus, Raf-1 is dispensable for the activation of the ERK pathway in fibroblasts and in the whole embryo.

We next monitored ERK activation in fibroblasts treated with apoptotic stimuli. ERK phosphorylation occurred normally in Raf-1-deficient cells treated with Fas antibody or with TNF-α (Figure 7).

A further downstream target of Raf-1 implicated in protection from apoptosis is the transcription factor NF-κB (Foo and Nolan, 1999). Raf-1 activates NF-κB by inducing I-κB phosphorylation and degradation. This pathway is distinct from MEK/ERK activation, but involves MEKK-1 upstream of the I-κB kinase complex (Baumann *et al*., 2000). Treatment of fibroblasts with TNF-α, but not with anti-Fas, caused rapid I-κB degradation, whose extent and kinetics were identical in c-*raf-1*$^{-/-}$ and c-*raf-1*$^{+/+}$ macrophages (Figure 7). Thus, Raf-1 is not essential for ERK

activation or I-κB degradation induced by these apoptotic stimuli.

Discussion

The c-*raf-1* gene is essential for mouse development, and its deletion leads to lethality at midgestation. On the 129/Sv and mixed 129BL/6 backgrounds, the organs mostly affected are the placenta and the liver. The placenta is reduced in size, and the labyrinth layer is poorly vascularized. A very similar phenotype has been observed in the placenta of Raf-1$^{-/-}$ outbred MF-1 mice (Hüser *et al*., 2001) and in *Craf-1*$^{neo2/neo2}$ outbred CD1 mice, which express a mutated 62 kDa Raf-1 protein with residual kinase activity (Wojnowski *et al*., 1998). Thus, both the loss and the N-terminal truncation of the Raf-1 kinase affect the development of this organ. While the placental defect probably plays a role in the growth retardation observed in Raf-1$^{-/-}$ embryos of different genetic backgrounds, most of the Raf-1$^{-/-}$/MF-1 and the *Craf-1*$^{neo2/neo2}$/CD1 mice reach term and die shortly after birth because of a failure of their lungs to inflate; however, most of their organs and tissues appear normal (Wojnowski *et al*., 1998).

Raf-1$^{-/-}$ livers of 129/Sv and mixed 129BL/6 backgrounds are pale, hypocellular and show increased apoptosis involving the hepatoblast compartment (Figures 2 and 3). On the outbred background, in contrast, hypocellularity and anemia are observed in the absence of overt fetal liver apoptosis (Hüser *et al*., 2001). Thus, the severity of the apoptotic phenotype depends on the genetic background. Intriguingly, the anomalies observed in Raf-1$^{-/-}$ livers of 129/Sv and mixed 129BL/6 backgrounds are reminiscent of the phenotype observed in mice deficient in K-Ras (Johnson *et al*., 1997), which is the most efficient Raf-1 activator (Yan *et al*., 1998; Voice *et al*., 1999) and the only Ras isoform essential for mouse development (Umanoff *et al*., 1995; Ise *et al*., 2000). The liver hypocellularity and the moderate increase in apoptosis observed in the K-Ras$^{-/-}$ and Raf-1$^{-/-}$ embryos suggest the continuous loss of limited numbers of highly proliferating precursor cells rather than the synchronous death of a large number of cells at a given developmental stage.

While the extent of liver apoptosis caused by the Raf-1$^{-/-}$ knock-out may vary depending on the genetic background, the anemic appearance is common to embryos of all investigated backgrounds. Consistently, fetal liver-derived Raf-1$^{-/-}$ multipotent hematopoietic cells cultured *in vitro* fail to accumulate. These cells exhibit a cell-autonomous survival defect, which fits with the previously reported negative effect of Raf-1 antisense oligomers on human hematopoietic precursors (Keller *et al*., 1996; Sanders *et al*., 1998). Interestingly, the Raf-1$^{-/-}$ cells are able to differentiate into mature erythrocytes *in vitro*, indicating that the mutation affects the survival of the precursor cell pool rather than their ability to differentiate (Z.Husak, E.Deiner, H.Beug and M.Baccarini, unpublished).

Raf activation has been postulated to impinge on the G_1 phase of the cell cycle via the ERK pathway (Brunet *et al*., 1999). However, we did not detect any significant defect in the proliferation of Raf-1$^{-/-}$ fetal liver cells *in vivo* and *in vitro*, and we could not find any cell cycle anomalies in the Raf-1$^{-/-}$ fibroblasts. Consistently, ERK activation is indistinguishable from the controls in whole-embryo extracts, in multipotent hematopoietic cells derived from the fetal liver (data not shown) and in primary Raf-1$^{-/-}$ fibroblasts. At least in the latter cells, it is likely that ERK activation would be mediated by B-Raf. These data are in agreement with previous reports identifying B-Raf as the major MEK activator in NIH 3T3 fibroblasts (Pritchard *et al*., 1995; Reuter *et al*., 1995) and in bovine brain (Catling *et al*., 1994; Yamamori *et al*., 1995). In Raf-1$^{-/-}$ cells, we observed a reproducible elevation (~2-fold) in the basal and EGF-induced activity of B-Raf as well as in basal MEK and ERK phosphorylation, suggesting the possibility that Raf-1 might have an inhibitory effect on B-Raf and its downstream effectors.

The anti-apoptotic function of Raf-1 appears to be responsible for the hypocellularity of Raf-1$^{-/-}$ fetal livers and for the reduced yield in cultures of Raf-1$^{-/-}$ fibroblasts and fetal liver-derived hematopoietic cells. In addition, Raf-1-deficient fibroblasts are more sensitive to apoptosis induced by a number of stimuli. The role of Raf-1 in apoptosis is controversial and, depending on the cell type and on the stimulus used, this kinase has been defined as a promotor (Blagosklonny *et al*., 1997; Kauffmann-Zeh *et al*., 1997; Basu *et al*., 1998) or as an inhibitor of apoptosis (Wang *et al*., 1994, 1996; Lau *et al*., 1998; Salomoni *et al*., 1998; Majewski *et al*., 1999; Peruzzi *et al*., 1999). The increased spontaneous apoptosis observed in c-*raf-1*$^{-/-}$ fetal livers *in vivo* and in cultured cells derived from c-*raf-1*$^{-/-}$ embryos, as well as the increased sensitivity of Raf-1$^{-/-}$ fibroblasts to stimulus-induced apoptosis, confirm the anti-apoptotic role of Raf-1, at least in the organ and in the cell types investigated. Stimulation of the ERK pathway by growth factors as well as by TNF-α or by Fas activation is not reduced by the absence of Raf-1. Therefore, effectors distinct from MEK/ERK must mediate this essential function of Raf-1. Consistent with this, the increased sensitivity to stimulus-induced apoptosis observed in Raf-1$^{-/-}$/MF-1 fibroblasts is rescued by a Raf-1 mutant devoid of growth factor-stimulated MEK kinase activity (Hüser *et al*., 2001).

The molecules mediating the anti-apoptotic function of Raf-1 are at present unknown. At least in fibroblasts, however, they can not be activated by B-Raf, which is present and active in these cells. The Raf kinases have been proposed to modulate mitochondrial integrity by regulating the activity of Bcl-2 family members (Wang *et al*., 1996; Salomoni *et al*., 1998; Peruzzi *et al*., 1999). In the specific case of Raf-1, stimulus-induced translocation of the kinase to the mitochondrial compartment (i.e. in proximity to the putative substrates) was demonstrated biochemically (Nantel *et al*., 1999; Peruzzi *et al*., 1999). More recent work, however, has demonstrated that the main Raf isoform associated with the mitochondrial compartment is A-Raf, while Raf-1 can not be detected in this compartment (Yuryev *et al*., 2000). A further downstream target of Raf-1 implicated in protection from apoptosis is the transcription factor NF-κB, particularly the RelA component (Lai *et al*., 1995; Baumann *et al*., 2000). The phenotype of mice lacking RelA (Beg and Baltimore, 1996; Doi *et al*., 1997) is somewhat reminiscent of the liver phenotype of the Raf-1$^{-/-}$ mice. However,

RelA ablation results in hypersensitivity towards TNF-α *in vivo* and *in vitro* (Beg and Baltimore, 1996; Doi *et al*., 1997), while Raf-1 ablation does not. In addition, TNF-α-induced I-κB degradation occurs normally in Raf-1-deficient cells. Therefore, it is very unlikely that NF-κB is the downstream target mediating the essential anti-apoptotic function of Raf-1.

In conclusion, our work and that of Hüser *et al*. (2001) show that the essential function of Raf-1 in the mouse embryo and in cultured cells is to prevent apoptosis rather than to promote proliferation, and that this function is not mediated by the MEK/ERK cascade. Defining the effectors involved in the anti-apoptotic function of Raf-1 is obviously a critical goal of future research. Furthermore, conditional ablation will allow us to circumvent embryonic lethality and to investigate the role of Raf-1 in the adult animal.

Materials and methods

Construction of the targeting vector

A genomic DNA clone containing a portion of Raf-1 was isolated from a 129/Sv mouse genomic λ fix library. An 8.5 kb 5′-*Xba*I–*Bgl*II-3′ fragment containing exon 3 and surrounding sequences was used to assemble the targeting construct in pBSIISK⁻. *loxP* sites were inserted as double-stranded oligonucleotides in the *Hin*dIII site 3′ of exon 3 and in the *Bam*HI site 5′ of exon 3. A *Neo*/*TK* cassette containing an upstream *loxP* site was excised from plasmid pGH1 and cloned into an *Xba*I–*Hin*dIII site contained in the *loxP* site 5′ of exon 3.

Electroporation and selection of ES cell clones

E14.1 ES cells grown on γ-irradiated embryonic fibroblasts were electroporated (260 V, 500 μF) with the *Asc*I-linearized targeting vector and selected with G418 (0.2 mg/ml). Homologous recombinants were obtained with a frequency of 1 in 35, as detected by nested PCR and Southern analysis. Positive clones were electroporated with a plasmid expressing the Cre recombinase (Gu *et al*., 1994). Cre expression led to deletion of either the floxed exon 3 or the floxed Neo/TK cassette, or both. The latter two were enriched by negative selection with gancyclovir. Two clones showing deletion between the most distant *loxP* sites were used to generate chimeras.

Generation of chimeras

C57BL/6 blastocyst stage embryos were injected with Raf-1$^{+/-}$ ES cells and then transferred to pseudopregnant B6CBAF1 mice for further development. Chimeric mice were mated to C57BL/6 and 129/Sv animals, and agouti offspring were genotyped. Germline transmission of the knock-out allele was detected by either Southern blot or PCR analysis of tail DNA.

PCR analysis of offspring and conceptuses

Tail and embryonic tissue DNA was prepared as described previously (Hilberg *et al*., 1993). Southern blot analysis (Southern, 1975) of *Pst*I-digested genomic DNA was performed using a probe located 3′ of exon 3 outside of the targeting vector (an ~750 bp *Bgl*II–*Xho*I fragment; Figure 1). The following primers were used for genotyping by PCR: 1, 5′-AACATGAAGTGGTGTTCTCCGGGCGCC-3′; 2, 5′-TGGCTG-TGTGCCCTTGGAACCTCAGCACC-3′; and 3, 5′-ATGCACTGAAAT-GAAAACGTGAAGACGACG-3′. Primers 1 and 2 amplify a 132 bp fragment of the endogenous allele, whereas primers 1 and 3 amplify a 320 bp fragment of the targeted allele.

Morphological, immunohistochemical and TUNEL analysis of placentas and fetuses

Embryos and corresponding placentas were dissected free of decidua and uterine muscle, and separated from the yolk sac. Two limb buds and the embryonic tail were saved for genotyping by PCR. For histology, embryos and placentas were fixed in 4% phosphate-buffered formaldehyde at 4°C for 16 h. After fixation, the tissues were dehydrated in graded solutions of alcohol and toluene, and infiltrated with paraffin (Histowax; Reichert-Jung, Vienna) at 58°C overnight, under vacuum. Sections (4–6 μm) were cut, mounted on silanized slides and stained with hematoxylin and eosin (Sigma Immunochemicals).

Immunohistochemistry was performed on 4-μm-thick sections of formaldehyde-fixed and paraffin-embedded E12.5 fetuses using a monoclonal rat antibody against TER119 (1:100; PharMingen), a polyclonal rabbit antibody against keratins 8 and 18 (Zatloukal *et al*., 1990) and a monoclonal anti-PCNA antibody (1:500; Dako).

An ultrasensitive avidin biotinylated enzyme complex (ABC) staining kit (Dako) was used on paraffin sections according to the protocol specified by the suppliers. Microwave pre-treatment in citric acid buffer was performed for all immunostainings. Control sections were treated with non-related isotype-matched immunoglobulin instead of primary antibody.

TUNEL was performed on paraffin sections using the *in situ* cell death detection kit (Roche). Slides were deparaffinized, and sections were digested with proteinase K (20 μg/ml) for 15 min at 37°C in the presence of fluorescein-labeled dUTP. Sections were counterstained with propidium iodide (1 μg/ml) for 2 min and then analyzed under the fluorescence microscope.

Cells and culture conditions

To obtain multipotent hematopoietic precursors, fetal liver cells were isolated from E11.5 129BL/6 fetuses, gently resuspended and expanded for 4–8 days in serum-free medium (StemPro34) supplemented with recombinant murine SCF (100 ng/ml), flk2/flt3 ligand (20 ng/ml), IL-3 (10 ng/ml), recombinant human IL-6 (5 ng/ml; all cytokines were from R&D systems), GM-CSF (1 ng/ml), insulin-like growth factor 1 (IGF-1; 40 ng/ml) and dexamethasone (Sigma). Cells were counted daily and diluted to maintain a constant density of 2×10^6 cells/ml. At day 4 and when mature cells accumulated in the cultures, proliferating, immature cells were purified by centrifugation through Ficoll 1.077 g/cm^2 (Kieslinger *et al*., 2000).

Primary mouse embryonic fibroblasts (MEFs) were isolated and immortalized as described (Todaro and Green, 1963). Each primary fibroblast culture was isolated from a single E 11.5–E12.5 mouse embryo of 129/Sv or 129BL/6 mixed genetic background, and each 3T3 fibroblast line was immortalized from an individual primary culture. Fibroblasts were cultured in Dulbecco's modified Eagle's medium supplemented with 10% fetal calf serum (FCS).

Cell cycle analysis and apoptosis assays

To obtain synchronized cells for cell cycle analysis, primary MEFs were arrested in G_0 by contact inhibition, followed by culture in medium containing 0.3% FCS for 48 h. Cells were released into the cell cycle by reseeding them at a standardized cell density in medium containing 20% FCS. DNA content was monitored by propidium iodide staining and flow cytometry using a Becton Dickinson FACScan system.

The number of cells in S phase in asynchronous cultures of hematopoietic precursors or of fibroblasts was determined using the *in situ* cell proliferation kit (Roche) according to the manufacturer's instructions, followed by microscopical examination of a randomly chosen area by independent experimenters. The number of apoptotic cells was determined using the *in situ* cell death detection kit (Roche) by staining with fluorescein isothiocyanate (FITC)-labeled annexin V (Clontech), followed by flow cytometry analysis (fetal liver cultures) or by microscopic analysis (fibroblasts) of randomly chosen areas of the sample by independent experimenters (300–500 cells/sample).

Apoptosis was induced in primary MEFs by cultivating the cells for 24 h in starvation media in the presence or absence of 20 ng/ml actinomycin D (Sigma). For Fas-induced apoptosis, 3T3-like fibroblasts were cultured in starvation medium containing 20 ng/ml actinomycin D and 50 ng/ml hamster anti-mouse Fas antibody (Jo2; PharMingen) for 22 h. For TNF-α-induced apoptosis, 3T3-like fibroblasts were treated with 100 ng/ml murine TNF-α (Calbiochem) alone or in combination with 5 μg/ml cycloheximide (Sigma) for 12 h. Measurements of cell death were performed using the CytoTox 96® Non-Radioactive Cytotoxicity Assay (Promega) according to the manufacturer's recommendations. Cell death was expressed as the percentage of maximum lactate dehydrogenase release.

Immunoprecipitation, assay of Raf kinase activity and western blot analysis

Primary MEFs were starved in medium containing 0.5% FCS for 18 h prior to stimulation with EGF (33 nM), 12-*O*-tetradecanoylphorbol-13-acetate (TPA; 100 nM) or FCS (20%). Cells were stimulated for 10 min, unless indicated otherwise. Cells or whole embryos were lysed in solubilization buffer (10 mM Tris–HCl, 50 mM NaCl, 1% Triton X-100,

30 mM sodium pyrophosphate, 100 μM Na_3VO_4, 1 mM phenylmethylsulfonyl fluoride). A rabbit polyclonal antiserum against a C-terminal peptide of v-Raf (SP63, CTLTTSPRLPVF) was used to immunoprecipitate Raf-1 molecules. A rabbit polyclonal antiserum (courtesy of Walter Kolch, Glasgow) was used to immunoprecipitate B-Raf molecules. Immunocomplexes were collected following incubation with protein A–Sepharose beads (Sigma). Raf kinase activity was measured as the ability of immunoisolated Raf-1 or B-Raf to activate recombinant MEK-1 in a coupled assay using myelin basic protein as the end point of the assay (Alessi *et al*., 1995). For western blotting, cell lysates (10–25 μg/lane) were separated by 12.5% SDS–PAGE prior to electrophoretic transfer onto Hybond C super (Amersham Pharmacia Biotech). The blots were probed with appropriate primary antibodies [Raf kinase domain (Kolch *et al*., 1990); B-Raf (Walter Kolch, Glasgow); MEK-1 (Transduction Laboratories); pMEK and pMAPK (New England Biolabs)] prior to incubation with peroxidase-conjugated secondary antibodies and detection by an enhanced chemiluminescence system (Pierce).

Acknowledgements

We thank Hans-Christian Theussl (IMP) for performing the blastocyst injections, Eva Deiner (IMP) for help with the hematopoietic cell cultures, Peter Steinlein (IMP) for help with the FACS analysis, Andrea Fuchsbichler (KFU Graz) for help with the immunohistochemistry, and Thomas Decker, Vienna Biocenter, for critical reading of the manuscript. This work was supported by the Austrian research Fund (grant P12279-MOB and P14230-MOB, to M.B.; grant S7401-MOB, to K.Z.; and grant S7406-MOB, to E.F.W.) and by grant PL963328 of the European Community (to M.B.).

References

Alessi,D.R., Cohen,P., Ashworth,A., Cowley,S., Leevers,S.J. and Marshall,C.J. (1995) Assay and expression of mitogen-activated protein kinase, MAP kinase kinase and Raf. *Methods Enzymol.*, **255**, 279–290.

Basu,S., Bayoumy,S., Zhang,Y., Lozano,J. and Kolesnick,R. (1998) BAD enables ceramide to signal apoptosis via Ras and Raf-1. *J. Biol. Chem.*, **273**, 30419–30426.

Baumann,B., Weber,C.K., Troppmair,J., Whiteside,S., Israel,A., Rapp,U.R. and Wirth,T. (2000) Raf induces NF-κB by membrane shuttle kinase MEKK1, a signaling pathway critical for transformation. *Proc. Natl Acad. Sci. USA*, **97**, 4615–4620.

Beg,A.A. and Baltimore,D. (1996) An essential role for NF-κB in preventing TNF-α-induced cell death. *Science*, **274**, 782–784.

Blagosklonny,M.V., Giannakakou,P., el-Deiry,W.S., Kingston,D.G., Higgs,P.I., Neckers,L. and Fojo,T. (1997) Raf-1/bcl-2 phosphorylation: a step from microtubule damage to cell death. *Cancer Res.*, **57**, 130–135.

Brunet,A., Roux,D., Lenormand,P., Dowd,S., Keyse,S. and Pouyssegur,J. (1999) Nuclear translocation of p42/p44 mitogen-activated protein kinase is required for growth factor-induced gene expression and cell cycle entry. *EMBO J.*, **18**, 664–674.

Catling,A.D., Reuter,C.W., Cox,M.E., Parsons,S.J. and Weber,M.J. (1994) Partial purification of a mitogen-activated protein kinase kinase activator from bovine brain. Identification as B-Raf or a B-Raf-associated activity. *J. Biol. Chem.*, **269**, 30014–30021.

Doi,T.S., Takahashi,T., Taguchi,O., Azuma,T. and Obata,Y. (1997) NF-κB RelA-deficient lymphocytes: normal development of T cells and B cells, impaired production of IgA and IgG1 and reduced proliferative responses. *J. Exp. Med.*, **185**, 953–961.

Foo,S.Y. and Nolan,G.P. (1999) NF-κB to the rescue: RELs, apoptosis and cellular transformation. *Trends Genet.*, **15**, 229–235.

Gu,H., Marth,J.D., Orban,P.C., Mossmann,H. and Rajewsky,K. (1994) Deletion of a DNA polymerase β gene segment in T cells using cell type-specific gene targeting. *Science*, **265**, 103–106.

Hilberg,F., Aguzzi,A., Howells,N. and Wagner,E.F. (1993) c-jun is essential for normal mouse development and hepatogenesis. *Nature*, **365**, 179–181.

Hüser,M. *et al*. (2001) MEK kinase activity is not necessary for Raf-1 function. *EMBO J.*, **20**, 1940–1951.

Johnson,L. *et al*. (1997) K-*ras* is an essential gene in the mouse with partial functional overlap with N-*ras*. *Genes Dev.*, **11**, 2468–2481.

Kauffmann-Zeh,A., Rodriguez-Viciana,P., Ulrich,E., Gilbert,C., Coffer,P., Downward,J. and Evan,G. (1997) Suppression of c-Myc-induced apoptosis by Ras signalling through PI(3)K and PKB. *Nature*, **385**, 544–548.

Keller,J.R., Ruscetti,F.W., Heidecker,G., Linnekin,D.M., Rapp,U., Troppmair,J., Gooya,J. and Muszynski,K.W. (1996) The effect of c-raf antisense oligonucleotides on growth factor-induced proliferation of hematopoietic cells. *Curr. Top. Microbiol. Immunol.*, **211**, 43–53.

Kieslinger,M., Woldman,I., Moriggl,R., Hofmann,J., Marine,J.C., Ihle,J.N., Beug,H. and Decker,T. (2000) Antiapoptotic activity of Stat5 required during terminal stages of myeloid differentiation. *Genes Dev.*, **14**, 232–244.

Kolch,W., Weissinger,E., Mischak,H., Troppmair,J., Showalter,S.D., Lloyd,P., Heidecker,G. and Rapp,U.R. (1990) Probing structure and function of the raf protein kinase domain with monoclonal antibodies. *Oncogene*, **5**, 713–720.

Lai,J.H., Horvath,G., Subleski,J., Bruder,J., Ghosh,P. and Tan,T.H. (1995) RelA is a potent transcriptional activator of the CD28 response element within the interleukin 2 promoter. *Mol. Cell. Biol.*, **15**, 4260–4271.

Lau,Q.C., Brusselbach,S. and Muller,R. (1998) Abrogation of c-Raf expression induces apoptosis in tumor cells. *Oncogene*, **16**, 1899–1902.

Majewski,M., Nieborowska-Skorska,M., Salomoni,P., Slupianek,A., Reiss,K., Trotta,R., Calabretta,B. and Skorski,T. (1999) Activation of mitochondrial Raf-1 is involved in the antiapoptotic effects of Akt. *Cancer Res.*, **59**, 2815–2819.

Marais,R., Light,Y., Paterson,H.F., Mason,C.S. and Marshall,C.J. (1997) Differential regulation of Raf-1, A-Raf and B-Raf by oncogenic ras and tyrosine kinases. *J. Biol. Chem.*, **272**, 4378–4383.

Marshall,M. (1995) Interactions between Ras and Raf: key regulatory proteins in cellular transformation. *Mol. Reprod. Dev.*, **42**, 493–499.

McCormick,F. (1995) Ras-related proteins in signal transduction and growth control. *Mol. Reprod. Dev.*, **42**, 500–506.

Morrison,D.K. and Cutler,R.E. (1997) The complexity of Raf-1 regulation. *Curr. Opin. Cell Biol.*, **9**, 174–179.

Nantel,A., Huber,M. and Thomas,D.Y. (1999) Localization of endogenous Grb10 to the mitochondria and its interaction with the mitochondrial-associated Raf-1 pool. *J. Biol. Chem.*, **274**, 35719–35724.

Naumann,U., Eisenmann-Tappe,I. and Rapp,U.R. (1997) The role of Raf kinases in development and growth of tumors. *Recent Results Cancer Res.*, **143**, 237–244.

Peruzzi,F., Prisco,M., Dews,M., Salomoni,P., Grassilli,E., Romano,G., Calabretta,B. and Baserga,R. (1999) Multiple signaling pathways of the insulin-like growth factor 1 receptor in protection from apoptosis. *Mol. Cell. Biol.*, **19**, 7203–7215.

Pritchard,C.A., Samuels,M.L., Bosch,E. and McMahon,M. (1995) Conditionally oncogenic forms of the A-Raf and B-Raf protein kinases display different biological and biochemical properties in NIH 3T3 cells. *Mol. Cell. Biol.*, **15**, 6430–6442.

Pritchard,C.A., Bolin,L., Slattery,R., Murray,R. and McMahon,M. (1996) Post-natal lethality and neurological and gastrointestinal defects in mice with targeted disruption of the A-Raf protein kinase gene. *Curr. Biol.*, **6**, 614–617.

Reuter,C.W., Catling,A.D., Jelinek,T. and Weber,M.J. (1995) Biochemical analysis of MEK activation in NIH3T3 fibroblasts. Identification of B-Raf and other activators. *J. Biol. Chem.*, **270**, 7644–7655.

Salomoni,P., Wasik,M.A., Riedel,R.F., Reiss,K., Choi,J.K., Skorski,T. and Calabretta,B. (1998) Expression of constitutively active Raf-1 in the mitochondria restores antiapoptotic and leukemogenic potential of a transformation-deficient BCR/ABL mutant. *J. Exp. Med.*, **187**, 1995–2007.

Sanders,M.R., Lu,H., Walker,F., Sorba,S. and Dainiak,N. (1998) The Raf-1 protein mediates insulin-like growth factor-induced proliferation of erythroid progenitor cells. *Stem Cells*, **16**, 200–207.

Schaeffer,H.J. and Weber,M.J. (1999) Mitogen-activated protein kinases: specific messages from ubiquitous messengers. *Mol. Cell. Biol.*, **19**, 2435–2444.

Southern,E.M. (1975) Detection of specific sequences among DNA fragments separated by gel electrophoresis. *J. Mol. Biol.*, **98**, 503–517.

Todaro,G.J. and Green,H. (1963) Quantitative studies of the growth of mouse embryo cells in culture and their development into established cell lines. *J. Cell Biol.*, **17**, 299–313.

Umanoff,H., Edelmann,W., Pellicer,A. and Kucherlapati,R. (1995) The murine N-*ras* gene is not essential for growth and development. *Proc. Natl Acad. Sci. USA*, **92**, 1709–1713.

Voice,J.K., Klemke,R.L., Le,A. and Jackson,J.H. (1999) Four human ras homologs differ in their abilities to activate Raf-1, induce transformation and stimulate cell motility. *J. Biol. Chem.*, **274**, 17164–17170.

Wang,H.G. *et al*. (1994) Apoptosis regulation by interaction of Bcl-2 protein and Raf-1 kinase. *Oncogene*, **9**, 2751–2756.

Wang,H.G., Rapp,U.R. and Reed,J.C. (1996) Bcl-2 targets the protein kinase Raf-1 to mitochondria. *Cell*, **87**, 629–638.

Wojnowski,L., Zimmer,A.M., Beck,T.W., Hahn,H., Bernal,R., Rapp,U.R. and Zimmer,A. (1997) Endothelial apoptosis in Braf-deficient mice. *Nature Genet.*, **16**, 293–297.

Wojnowski,L., Stancato,L.F., Zimmer,A.M., Hahn,H., Beck,T.W., Larner,A.C., Rapp,U.R. and Zimmer,A. (1998) Craf-1 protein kinase is essential for mouse development. *Mech. Dev.*, **76**, 141–149.

Yamamori,B., Kuroda,S., Shimizu,K., Fukui,K., Ohtsuka,T. and Takai,Y. (1995) Purification of a Ras-dependent mitogen-activated protein kinase kinase kinase from bovine brain cytosol and its identification as a complex of B-Raf and 14-3-3 proteins. *J. Biol. Chem.*, **270**, 11723–11726.

Yan,J., Roy,S., Apolloni,A., Lane,A. and Hancock,J.F. (1998) Ras isoforms vary in their ability to activate Raf-1 and phosphoinositide 3-kinase. *J. Biol. Chem.*, **273**, 24052–24056.

Yuryev,A., Ono,M., Goff,S.A., Macaluso,F. and Wennogle,L.P. (2000) Isoform-specific localization of A-RAF in mitochondria. *Mol. Cell. Biol.*, **20**, 4870–4878.

Zatloukal,K., Denk,H., Spurej,G., Lackinger,E., Preisegger,K.H. and Franke,W.W. (1990) High molecular weight component of Mallory bodies detected by a monoclonal antibody. *Lab. Invest.*, **62**, 427–434.

Received January 2, 2001; revised January 31, 2001;
accepted February 6, 2001